Adsorption at Liquid Interfaces Induces Amyloid Fibril Bending and Ring Formation — Supporting Information —

Sophia Jordens,[1] Emily E. Riley,[2,3] Ivan Usov,[1] Lucio Isa,[4,5] Peter D. Olmsted,[2,6,*] and Raffaele Mezzenga[1,*]

[1] *ETH Zurich, Department of Health Sciences & Technology, Laboratory of Food & Soft Materials, 8092 Zurich, Switzerland*
[2] *University of Leeds, School of Physics & Astronomy, Soft Matter Physics Group, Leeds LS2 9JT, United Kingdom*
[3] *Current address: Cambridge University, Department of Applied Mathematics and Theoretical Physics, Cambridge CB3 0WA, United Kingdom*
[4] *ETH Zurich, Department of Materials, Laboratory for Surface Science & Technology, 8093 Zurich, Switzerland*
[5] *Current address: ETH Zurich, Department of Materials, Laboratory for Interfaces, Soft Matter & Assembly, 8093 Zurich, Switzerland*
[6] *Current Address: Georgetown University, Department of Physics and Institute for Soft Matter Synthesis & Metrology, Washington DC 20057, USA*

(Dated: October 21, 2014)

1. PERSISTENCE OF RINGS IN THE PRESENCE OF NEMATIC DOMAINS

Rings can be observed even at high interfacial fibril densities, where nematic domains cover most of the observed area as shown in Fig. S1 and S2. At this point, the rings are usually composed of many fibrils or are completely filled by short fibrils. It is worth noting, however, that some regions on the same sample can be void of rings. There is a population of fibrils in all four batches investigated that is not consistent with the height and pitch distributions observed in [1]. These fibrils are very tightly wound with a half-pitch length around 40 nm and a maximum height between 4 and 7 nm and can also be seen to partake in ring formation.

2. SPONTANEOUS BENDING OF A POLAR TWISTED RIBBON AT AN INTERFACE

A. Surface Interaction

Most particles, including proteins, adsorb to a hydrophobic-hydrophilic interface in order to reduce the nascent hydrophobic surface tension [2]. In addition to this, a protein will interact specifically with the two media according to the nature of the amino acids. Such interactions are both short-range (charge, hydrophobic effect, steric shapes) and long-range (dispersion interactions) [3]. Long range interactions depend weakly on the nature of the surface, as they typically include the bulk of the two interface materials and the entire protein. However, the short range surface interactions depend critically on the details of the surface of the protein. The inhomogeneous surface of a protein results in a local moment or torque applied by the fluid at each point on the surface. For a helical protein immersed in a homogeneous fluid, this local torque will sum to zero across the entire surface of the protein. However, for a protein in an inhomogeneous environment, such as one confined to an interface, will experience a non-zero total torque $\mathbf{\Gamma}$. This can induce a spontaneous curvature or twist depending on both the direction of $\mathbf{\Gamma}$ and the strength of the intrinsic bend and twist moduli.

The net torque on the protein due to its environment can be separated into contributions from short range and long range forces:

$$\mathbf{\Gamma} = \int_V d^3r\, \mathbf{r} \times \mathbf{f}_{LR}(\mathbf{r}) + \Delta \int_S d^2r\, \mathbf{r} \times \mathbf{f}_{SR}(\mathbf{r}, z)\,, \tag{1}$$

where S and V are respectively the surface and volume of the protein. The force densities are given by

$$\mathbf{f}(\mathbf{r}) = -\int_{\text{env}} d^3r'\, \frac{\partial \mathcal{U}\,(\mathbf{r}-\mathbf{r}')}{\partial(\mathbf{r}-\mathbf{r}')}, \tag{2}$$

*To whom correspondence may be addressed. Email: pdo7@georgetown.edu, raffaele.mezzenga@hest.ethz.ch

where the energy density $\mathcal{U}(\mathbf{r}-\mathbf{r}')$ of interaction (energy per volume squared) between material in the environment at $\mathbf{r}'$ and in the protein at $\mathbf{r}$ can be separated into long range (*e.g.* dispersion or Coulomb) and short-range (*e.g.* hydrophobic or steric) interactions. Here, Δ is the interaction depth within the protein (of order an amino acid in size), and the forces are obtained by integrating over points $\mathbf{r}'$ in the environment external to the protein. Although the net torque will generally depend on the entire shape and volume of the protein (because of long range dispersion and Coulomb interactions), we will illustrate the example where the effects of long range forces are negligible compared to those of the short range interactions. For example, an unbalanced torque that leads to a bend in the plane of the interface will not perturb the long range energy of interaction appreciably, since there will be neligible response perpendicular to the interface.

In the case of short range interactions, we can approximate the integral over the environment as $\int_{\text{env}} d^3r' \simeq a \int dz'$, where the coordinate z' is along the surface normal and a is the lateral area of the short interaction. By integrating the short range potential and using the reference $\mathcal{U}(z=\infty)=0$, we can write the torque exerted on the surface as

$$\mathbf{\Gamma} = a\Delta \int_S d^2r\,(\mathbf{r}\times\hat{\mathbf{n}})\,\mathcal{U}(\mathbf{r}), \tag{3}$$

$$\equiv \int_S d^2r\,(\mathbf{r}\times\hat{\mathbf{n}})\,\left[\bar{\gamma}+\delta\gamma\,(\mathbf{r})\right], \tag{4}$$

The quantity $(a\Delta)\mathcal{U}(\mathbf{r}) \equiv \bar{\gamma}+\delta\gamma(\mathbf{r})$ is the surface energy density of interaction introduced in Eq. [3] of the main text.

Fluid-fluid interface – At fluid-fluid interfaces an adsorbed fibril will be surrounded by both fluids, according to the (inhomogeneous) degree of wettability of the fibril on the two fluids. This inhomogeneous environment leads to a net uncompensated moment when averaged over the inhomogenous solvent environment around the fibril. Although this applies to the problem at hand, we will take the a pragmatic approach and illustrate the method for the simpler example of a fluid-solid interface with short-range interactions.

Fluid-solid interface – Consider a fibril adsorbed to a fluid-solid interface. Material within a short range Δ, set by Coulomb screening, shapes of asperities, or hydrophobic effects, will interact with the solid substrate on a strip. For short range interactions a surface interaction that is symmetric from head to tail (a non-polar interaction) will lead to zero applied total torque, as the local torque will sum to zero, as in a homogeneous environment. However, a non-symmetric interaction will lead to uncompensated torques, or bending moments, all along the length of the adsorbed fibril.

B. Twisted Ribbon of Fixed Radius

To make progress, we approximate the fibril of length L as a twisted ribbon with wavelength λ, which makes contact every half wavelength with a solid surface on the exposed edges at the ribbon radius R (Figures S5, S6). The wavelength is related to the helical angle θ_p by

$$\cos\theta_p = \frac{qR}{\sqrt{1+(qR)^2}} \qquad\qquad \sin\theta_p = \frac{1}{\sqrt{1+(qR)^2}}, \tag{5}$$

where $q = 2\pi/\lambda$. The centerline of the undeformed fibril defines a tangent vector $\hat{\mathbf{t}}_0$, which upon bending becomes $\hat{\mathbf{t}}(s)$, with local curvature $\kappa = |d\hat{\mathbf{t}}/ds| \equiv |\dot{\hat{\mathbf{t}}}|$. Equivalently, we can parametrize the curvature in terms of the vector angular rotation of the tangent vector, defined by $\dot{\mathbf{\Theta}} = \hat{\mathbf{t}}\times\dot{\hat{\mathbf{t}}}$.

Rather than work in terms of torques exerted across the body, we will calculate the surface energy of the adsorbed fibril as a function of the fibril shape. Minimizing this energy with respect to in-plane bending will lead to an induced spontaneous curvature, which is equivalent to finding an uncompensated torque for a straight fibril.

For a small interaction range, $\Delta \ll R$, the interaction between the surface and the twisted ribbon can be approximated by the surface energy of series of strips of thickness $\omega = 2\sqrt{2R\Delta-\Delta^2} \simeq \sqrt{8R\Delta}$ (Fig. S5). The ribbon-surface energy is given by

$$G_{\text{surf}} = \sum_{j=1}^{2L/\lambda} \int_{S_j} \left[\bar{\gamma}+\delta\gamma(\mathbf{r})\right] d^2r \tag{6}$$

$$\equiv \sum_{j=1}^{2L/\lambda} G_{\text{polar},j}, \tag{7}$$

where S_j is the surface area of the jth interaction strip, the average surface energy $\bar{\gamma}$ represents the absorption properties of the ribbon, and $\delta\gamma$ captures the polar nature of the interaction. There are $2L/\lambda$ distinct interaction strips. We assume that the strip has an anisotropic interaction potential that is polar along the direction $\hat{\mathbf{u}}$ within the strip, and assume the simple form

$$\delta\gamma(\mathbf{r}) = \varepsilon\, \mathbf{r}\cdot\hat{\mathbf{u}} \tag{8a}$$
$$= \varepsilon\,(x\cos\Phi + y\sin\Phi)\,, \tag{8b}$$

where $\hat{\mathbf{u}}$ is at an angle Φ with respect to the tangent vector $\hat{\mathbf{t}}$.In the limit of $R \gg \Delta$ the strips can be approximated as flat, taking $\mathbf{r}$ as a two-dimensional vector in the plane of the surface. For short range interactions these flat strips constitute the primary interaction between the surface and the twisted ribbon.

Amyloid fibrils are composed of protofilaments, which in turn comprise layers of aligned beta sheets that are twisted about their central axis. A given fibril contains a number of protofilaments that form a ribbon, which we approximate as shown in Figure S6(A). The ribbon diameter D is given by the number of protofilaments in the fibrils, while the ribbon thickness d is determined by the diameter of an individual protofilament. The ribbon length L is determined by the total number of aligned beta strands.

For an undeformed fibril the interaction strip is a parallelogram tilted at an angle θ_p determined by the pitch of the ribbon, and with lengths determined by the thickness d of the ribbon (the perpendicular distance between the edges) and the strip thickness ω, as shown in Figure S6(B). Two sides of length $\ell = d/\sin\theta_p$ are parallel to the tangent vector $\hat{\mathbf{t}}_0$, while the other two sides have length $\omega/\cos\theta_p$.

When the ribbon is bent the ribbon thickness d is fixed due to the fixed radius, but it curves to follow the deformed tangent vector $\hat{\mathbf{t}}$. Given that we are in the small bend regime, we approximate these sides as straight, but tilted additionally by $\bar{\phi} = \frac{1}{2}(\phi_R + \phi_L)$ according to the average tilt of the interaction strip (Figure S6(C)). Here ϕ_L and ϕ_R represent the additional tilts on the left and right hand sides of the interaction strip.

When the strip is bent downwards the top of the interaction strip is under tension whereas the bottom of the strip is under compression. Although the center of the strip is not under tension or compression, bend-stretch coupling terms may cause the ribbon to stretch or compress, leading to a new strip length $\ell' = d/\sin(\theta_p - \bar{\phi})$. This change in length contributes to the bend-stretch coupling, which is not of interest here.

Initially, the polarity vector $\hat{\mathbf{u}}_0$ is at an angle Φ with respect to the tangent vector $\hat{\mathbf{t}}_0$. When the twisted ribbon is bent, then to first order the all vectors in the interaction strip rotate with the average rotation $\bar{\phi}$ of a particular segment; this includes both the polarity vector and the local tangent vector. However, the stretching and compression on either side of the bend cause the polarity vector to deflect non-affinely aross the strip; e.g the tilt of the polarity vector should vary smoothly between ϕ_L and ϕ_R, when moving from left to right across the strip. For simplicity we will take the polarity vector to be tilted by $\bar{\phi}$ everywhere on the interaction strip. With this notation, the polar surface potential becomes

$$\delta\gamma(\mathbf{r})|_{\text{bent}} = \varepsilon\left[x\cos(\Phi - \bar{\phi}) + y\sin(\Phi - \bar{\phi})\right]. \tag{9}$$

C. Polar Free Energy

The polar energy across a single interaction strip, or equivalently the energy per helical repeat, is then given by

$$G_{\text{polar}} = \varepsilon \int_{-\frac{1}{2}\omega}^{\frac{1}{2}\omega} dy \int_{f_L(y)}^{f_R(y)} dx\left[x\cos\left(\Phi - \bar{\phi}\right) + y\sin\left(\Phi - \bar{\phi}\right)\right], \tag{10}$$

where

$$f_L(y) = y\cot[\theta_p + \tfrac{1}{2}(\phi_R - \phi_L)] - \tfrac{1}{2}\ell \tag{11}$$
$$f_R(y) = y\cot[\theta_p - \tfrac{1}{2}(\phi_R - \phi_L)] + \tfrac{1}{2}\ell\,, \tag{12}$$

and ℓ is the length of center of the interaction strip parallel to $\hat{\mathbf{t}}_0$. This evaluates to

$$G_{\text{polar}} = \frac{\varepsilon\omega^3}{12}\left[\cot\left(\theta_p - \tfrac{1}{2}\Theta\right) - \cot\left(\theta_p + \tfrac{1}{2}\Theta\right)\right]\left\{\sin\left(\Phi - \bar{\phi}\right) + \tfrac{1}{2}\cos\left(\Phi - \bar{\phi}\right)\left[\cot\left(\theta_p - \tfrac{1}{2}\Theta\right) + \cot\left(\theta_p + \tfrac{1}{2}\Theta\right)\right]\right\}, \tag{13}$$

where $\Theta = \phi_R - \phi_L$ is the angular deflection associated with the bend. The energy of deformation vanishes for zero bend $\Theta = 0$. A positive bend $\Theta > 0$ corresponds to a right hand bend, when travelling parallel to the chosen direction fo the tangent vector.

Our goal is to study the lowest order effects of the surface, which induce a spontaneous curvature signified by the term linear in bend Θ that arises from the small Θ approximation to G_{polar}. The average tilt $\bar{\phi}$ can be related, geometrically, to a combination of twist and stretch, which leads to surface-induced bend-twist and bend-stretch couplings. Thus, we will expand Eq. 13 to first order in Θ, and set $\bar{\phi} = 0$ because we are not interested in higher order bend-twist or bend-stretch couplings (the effects of these would only be visible upon observing changes in total fibril length, or in local chirality). To lowest order in the deflection we find

$$G_{\text{polar}} = \frac{\varepsilon\omega^3}{12\sin^2\theta_p}(\cos\Phi\cot\theta_p + \sin\Phi)\,\Theta + \dots \tag{14}$$

$$\simeq \frac{\varepsilon\omega^3\ell}{12\sin^2\theta_p}(\cos\Phi\cot\theta_p + \sin\Phi)\,\frac{d\Theta}{ds}. \tag{15}$$

In performing this expansion we have assumed that the polar direction $\hat{\mathbf{u}}$ (or Φ) rotates affinely with the tangent; deviations from this will lead to higher order couplings $\Theta\,\delta\Phi$. Hence, the contribution to the bending energy of the entire fibril is

$$G_{\text{surf}} = \sum_{j=1}^{2L/\lambda} G_{\text{polar},j} \tag{16}$$

$$= \int_0^L \frac{2\,ds}{\lambda}\frac{\varepsilon\omega^3\ell}{12\sin^2\theta_p}(\cos\Phi\cot\theta_p + \sin\Phi)\,\frac{d\Theta}{ds}, \tag{17}$$

where we have assumed that the bend is smooth between contacts, and converted the sum to an integral via $\sum_j \to \int ds/\lambda$.

The polar moment is given by

$$\mathbf{P} = \frac{2}{\lambda}\int_S \mathbf{r}\,\delta\gamma(\mathbf{r})\;d^2r, \tag{18}$$

$$= \frac{2\varepsilon}{\lambda}\int_S \mathbf{r}\,(\mathbf{r}\cdot\hat{\mathbf{u}})\;d^2r, \tag{19}$$

$$= \frac{\varepsilon}{\lambda}\frac{\partial}{\partial\hat{\mathbf{u}}}\int_{-\frac{\omega}{2}}^{\frac{\omega}{2}} dy \int_{y\cot\theta_p-\frac{\ell}{2}}^{y\cot\theta_p+\frac{\ell}{2}} [x\cos\Phi + y\sin\Phi]^2\;dx \tag{20}$$

$$= \frac{\varepsilon\omega^3\ell}{6\lambda}\left\{\left[\cos\Phi\left(\cot^2\theta_p + \left(\frac{\ell}{\omega}\right)^2\right) + \sin\Phi\cot\theta_p\right]\hat{\mathbf{t}} + (\sin\Phi + \cos\Phi\cot\theta_p)\,\hat{\mathbf{n}}\times\hat{\mathbf{t}}\right\}. \tag{21}$$

One component of $\mathbf{P}$ is parallel to the fibril direction $\hat{\mathbf{t}}$, while the other direction is perpendicular to $\hat{\mathbf{t}}$ and in the plane specified by normal vector $\hat{\mathbf{n}}$. Note that $\{\hat{\mathbf{t}}, \hat{\mathbf{n}}\times\hat{\mathbf{t}}, \hat{\mathbf{n}}\}$ form an orthonormal basis. Hence,

$$\mathbf{P} = P_\parallel\mathbf{t} + P_\perp\hat{\mathbf{n}}\times\hat{\mathbf{t}}, \tag{22}$$

where

$$P_\parallel = \frac{\varepsilon\omega^3\ell}{6\lambda}\left[\cos\Phi\left(\cot^2\theta_p + \left(\frac{\ell}{\omega}\right)^2\right) + \sin\Phi\cot\theta_p\right] \tag{23a}$$

$$P_\perp = \frac{\varepsilon\omega^3\ell}{6\lambda}\left(\sin\Phi + \cos\Phi\cot\theta_p\right). \tag{23b}$$

Comparing the definition of $\mathbf{P}$ with the free energy G_{surf}, we can rewrite the surface energy as

$$G_{\text{surf}} = \frac{1}{\sin^2\theta_p}\int_0^L ds\,P_\perp\,\frac{d\Theta}{ds}. \tag{24}$$

In vector form, the angular rotation is given by $\dot{\mathbf{\Theta}} = -\hat{\mathbf{n}}\frac{d\Theta}{ds}$ (Fig. S6), while the component $P_\perp$ can be extracted via $P_\perp = \hat{\mathbf{n}}\cdot\hat{\mathbf{t}}\times\mathbf{P}$. Thus, the free energy becomes

$$G_{\text{surf}} = -\frac{1}{\sin^2\theta_p}\int_0^L ds\,\dot{\mathbf{\Theta}}\cdot\hat{\mathbf{t}}\times\mathbf{P}, \tag{25}$$

which corresponds to the free energy of Equations 5-6 in the main text, with $A = 1/\sin^2\theta_p$.

D. Induced Curvature

The total bending free energy is given by the sum of the standard bending energy and the coupling to the surface:

$$G_{bend} = \int ds \left[\frac{1}{2} B \dot{\mathbf{\Theta}}^2 - \frac{1}{\sin^2 \theta_p} \dot{\mathbf{\Theta}} \cdot \hat{\mathbf{t}} \times \mathbf{P} \right] \tag{26}$$

$$= \int ds \left[\frac{1}{2} B \kappa^2 - \frac{\varepsilon \omega^3 \ell}{6 \lambda \sin^2 \theta_p} (\cos \Phi \cot \theta_p + \sin \Phi) \kappa \right], \tag{27}$$

where the (signed) curvature is defined by $\dot{\Theta} = \kappa \hat{\mathbf{n}}$. The bending modulus generally includes contributions from the surface, which can be calculated based on the formalism here. However, since our intent is to demonstrate the significance of the induced curvature, we do not consider such perturbations. Moreover, the main contribution to bending is usually from internal degrees of freedom that are only weakly influenced by the surface. An exception occurs for highly charged filaments. In such cases the reduction in the dielectric constant and lack of screening near a hydrophobic surface will increase the electrostatic contribution to B.

This bend energy is minimized by the following spontaneous curvature κ_0:

$$\kappa_0 = \frac{\varepsilon \omega^3 \ell}{6 \lambda \sin^2 \theta_p B} (\cos \Phi \cot \theta_p + \sin \Phi) \tag{28}$$

$$= \frac{\varepsilon \omega^3 \ell}{\lambda \sin^2 \theta_p B} \alpha(\theta_p, \Phi), \tag{29}$$

where $\alpha(\theta_p, \Phi) \equiv (\cos \Phi \cot \theta_p + \sin \Phi)/6$.

The sign of the induced curvature can be understood as follows. Consider $\varepsilon > 0$, a helix with an opening angle of $\theta_p = \pi/4$, and a polarization direction specified by $\Phi = \pi/6$ (roughly as in Figs. S5, S6). In this case there is a higher energy for exposing the upper right part of the parallelogram in Fig. S6 to the surface. Hence the preferred bending direction should be 'up' in Fig. S5 (rather than the downward shown), to allow the relatively less of the costly part of the surface interaction to attain more contact with the surface. This corresponds to a positive bend around $\hat{\mathbf{n}}$, given by $\dot{\mathbf{\Theta}} = \kappa_0 \hat{\mathbf{n}}$ with $\kappa_0 > 0$ and matches the prediction in Eq. (28).

---

[1] Adamcik, J. *et al.* Understanding Amyloid Aggregation by Statistical Analysis of Atomic Force Microscopy Images. *Nature Nanotech.* **2010**, *5*, 5423–428.

[2] Pickering, S. CXCVI.—Emulsions. *J. Chem. Soc., Trans.* **1907**, *91*, 2001–2021.

[3] Israelachvili, J.N. *Intermolecular and Surface Forces* Academic Press: London, 1992).

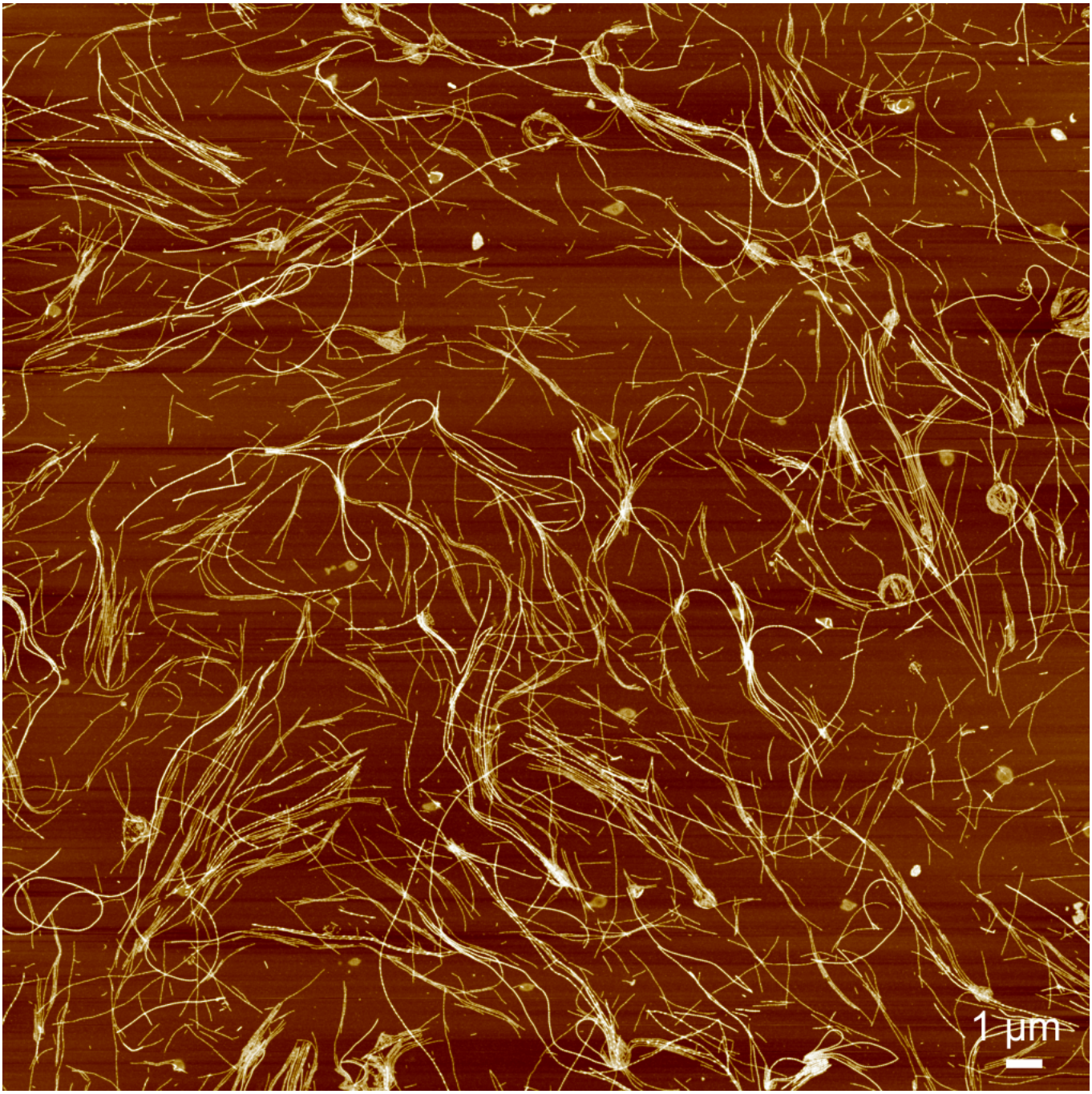

FIG. S1: AFM image of fibrils at the air-water interface after t=60 minutes adsorption time from a $c_{\mathrm{init}} = 0.001\%$ w/w fibril suspension.

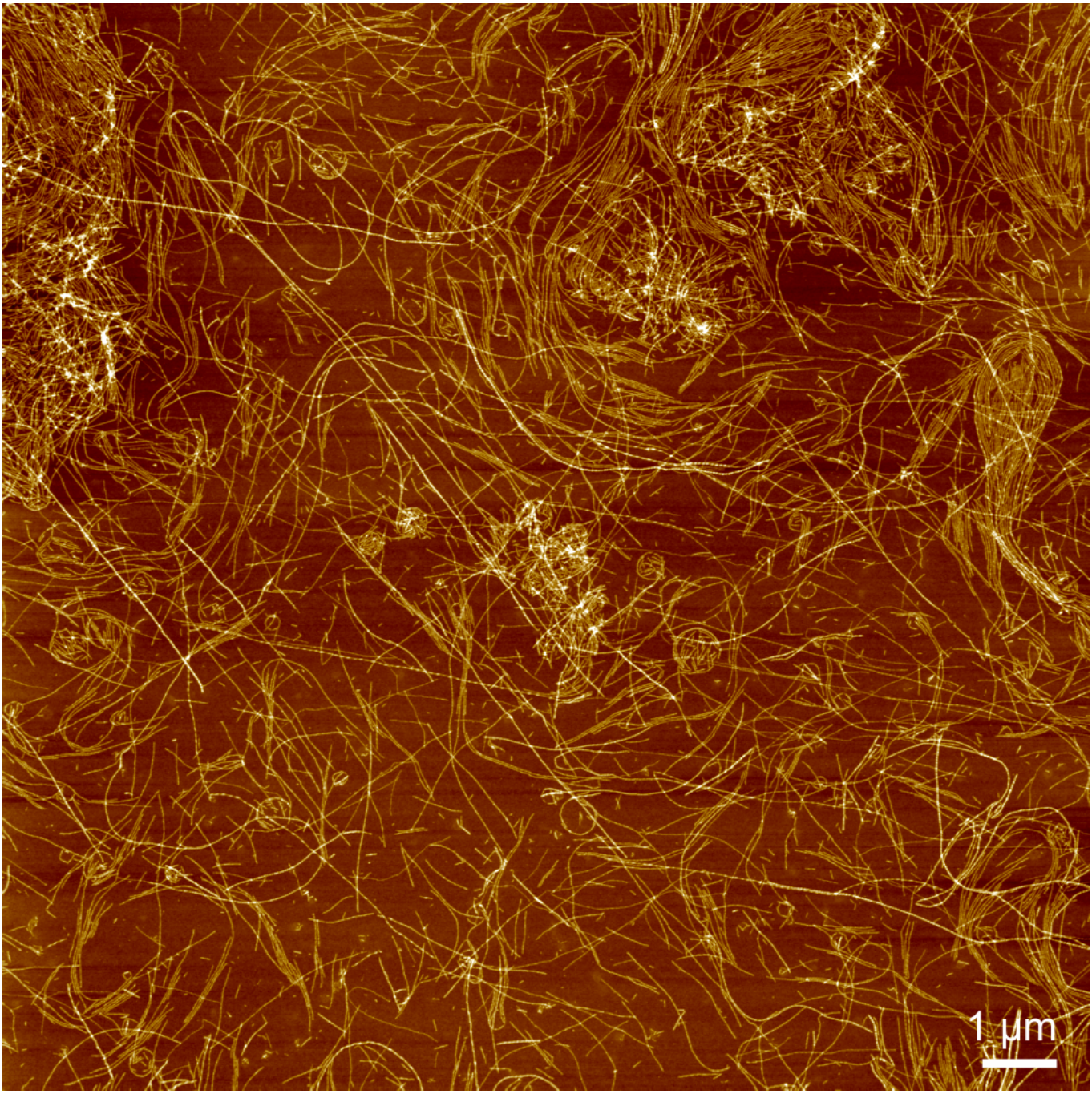

FIG. S2: AFM image of fibrils at the air-water interface after t=10 minutes adsorption time from a $c_{\mathrm{init}} \approx 0.008\%$ w/w fibril suspension. Rings coexist with nematic fibril domains.

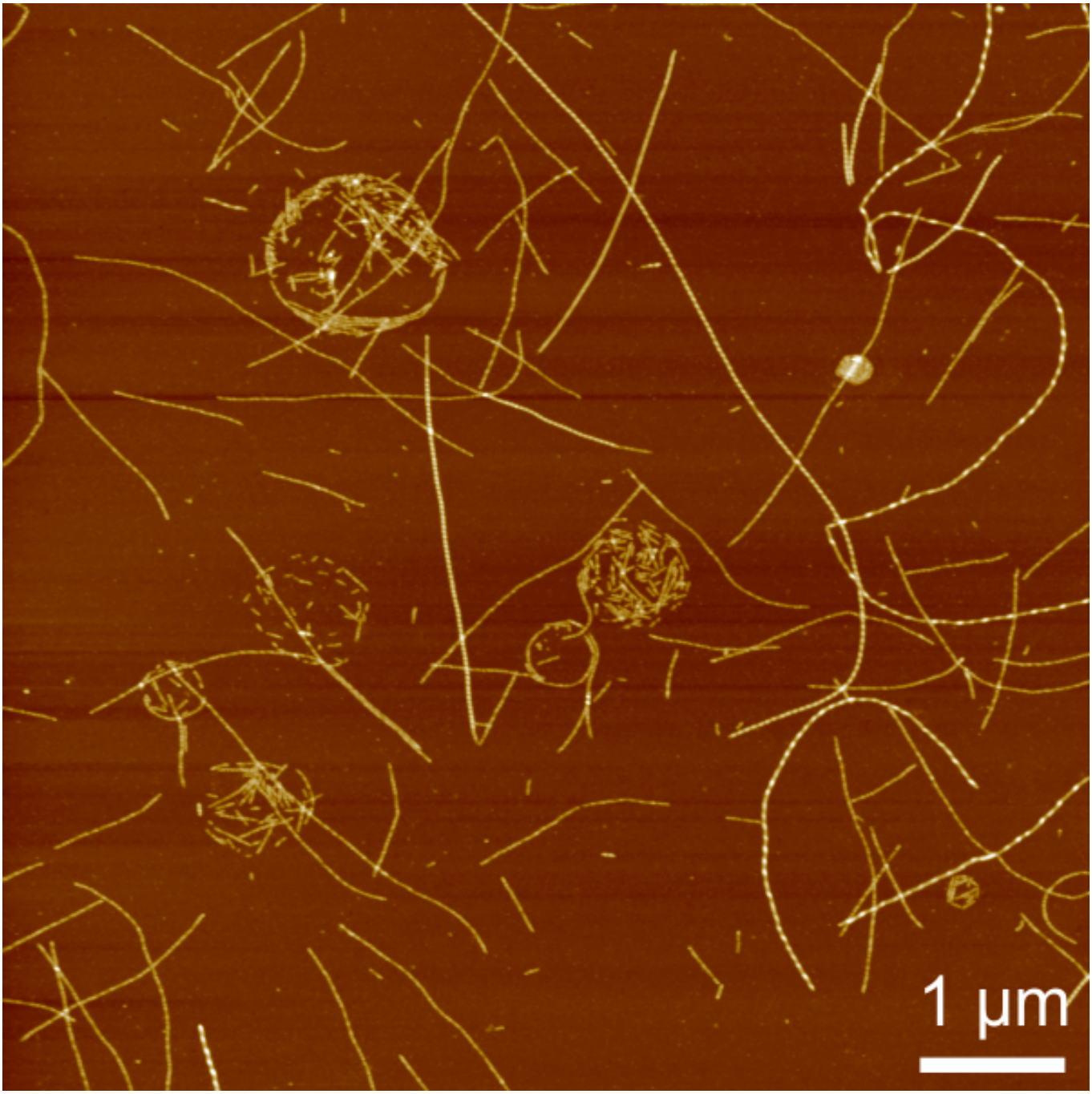

FIG. S3: AFM image of fibrils at the air-water interface after t=60 minutes adsorption time from a $c_{\mathrm{init}} = 0.001\%$ w/w fibril suspension. Rings are often composed of many short fibrils.

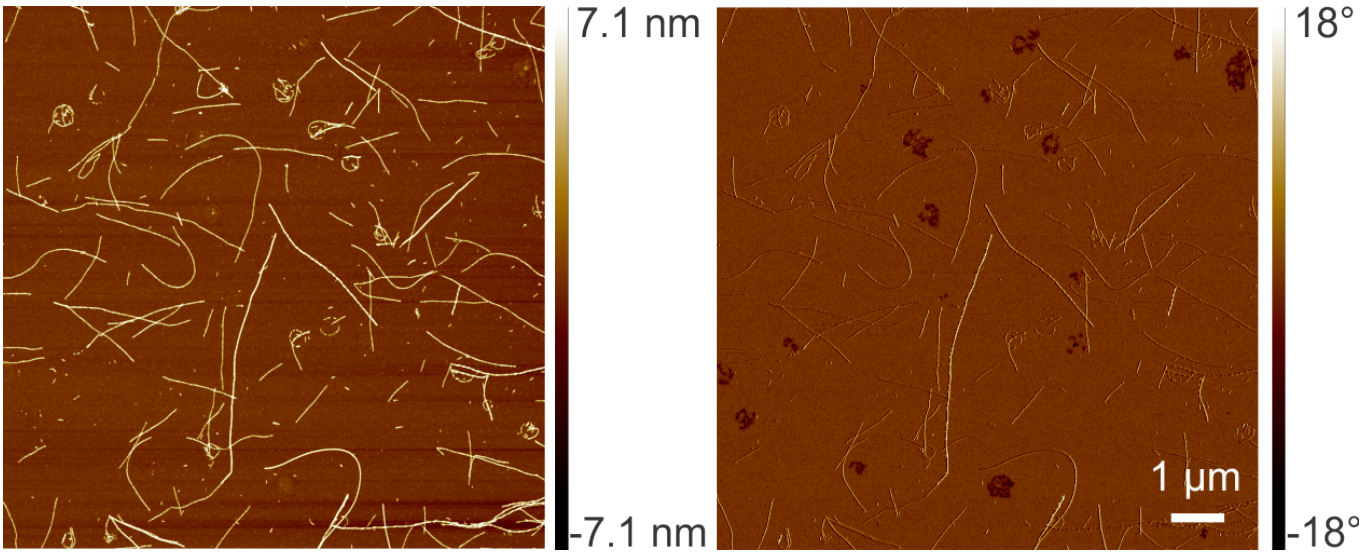

FIG. S4: AFM height and phase images of fibrils at the air-water interface immediately after sample preparation of a $c_{\text{init}} = 0.001\%$ w/w fibril suspension. The scale bar applies to both images. Distortions in the background peptide layer are readily visible in the phase image but are rarely spherical and do not coincide spatially with fibril rings.

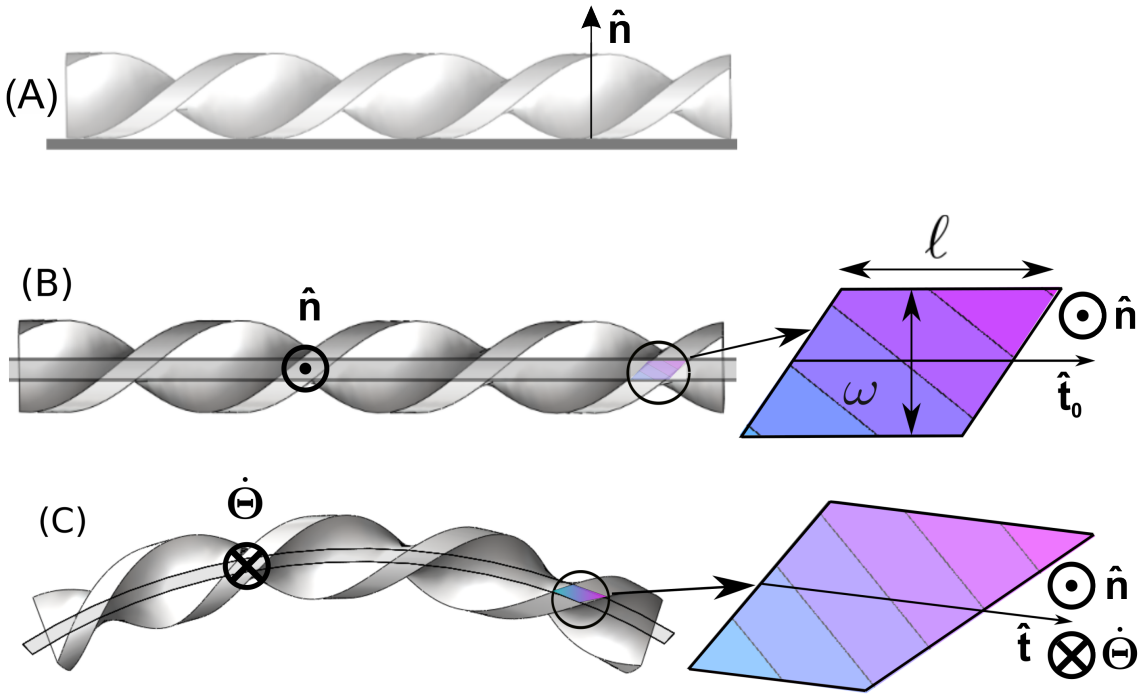

FIG. S5: (A) Helical fibril against a surface. (B) The contact area, or interaction strip, is a parallelogram that deforms asymmetrically (C) when the fibril is bent. This leads to an excess contact area by one 'charge' of the polar interaction, leading to a preference for one sign of bend and thus a spontaneous curvature. A positive red 'charge' and a negative 'blue' charge corresponds to a polarization potential $\delta\gamma = \varepsilon(\cos\pi/6 + y\sin\pi/6)$, with $\varepsilon > 0$. In this case the bend shown in (C) costs energy, and the preferred spontaneous curvature instead correponds to a bend $\frac{d\mathbf{\Theta}}{ds} = \dot{\mathbf{\Theta}} = \hat{\mathbf{t}} \times \dot{\hat{\mathbf{t}}}$ which is parallel to $\hat{\mathbf{n}}$.

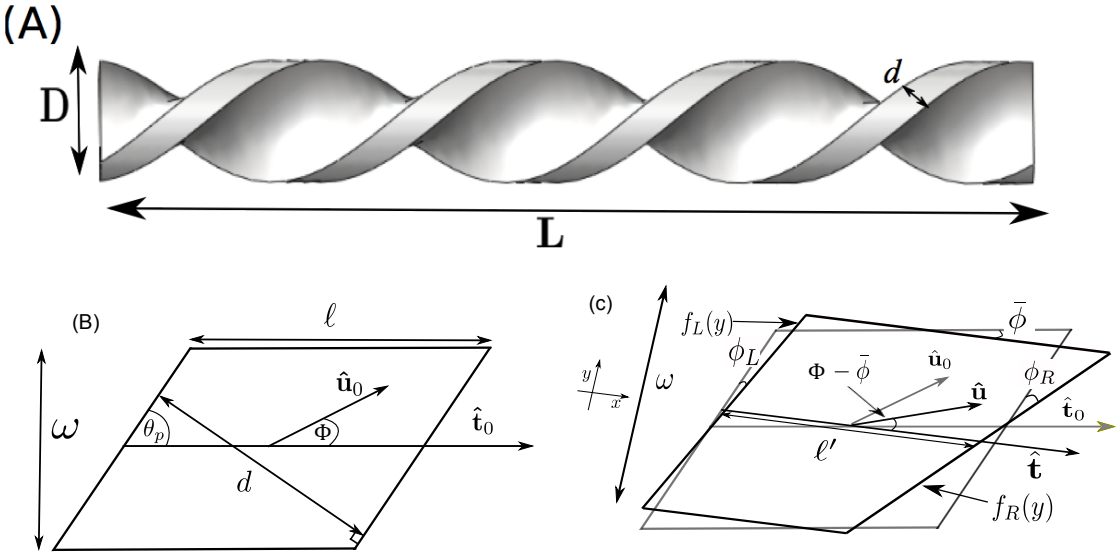

FIG. S6: (A) Geometry of twisted ribbon. Initial (B) and deformed (C) interaction strips, obtained by bending the fibril. The undeformed strip is shown in grey under the deformed strip. The bend causes a tilt in the two sides (right and left) depending on the change in the tangent vector across the strip, while the top and bottom sides remain parallel to each other, but rotate with respect to the undeformed strip by $\bar{\phi} = \frac{1}{2}(\phi_L + \phi_R)$, which describes the average tilt of the individual strip.

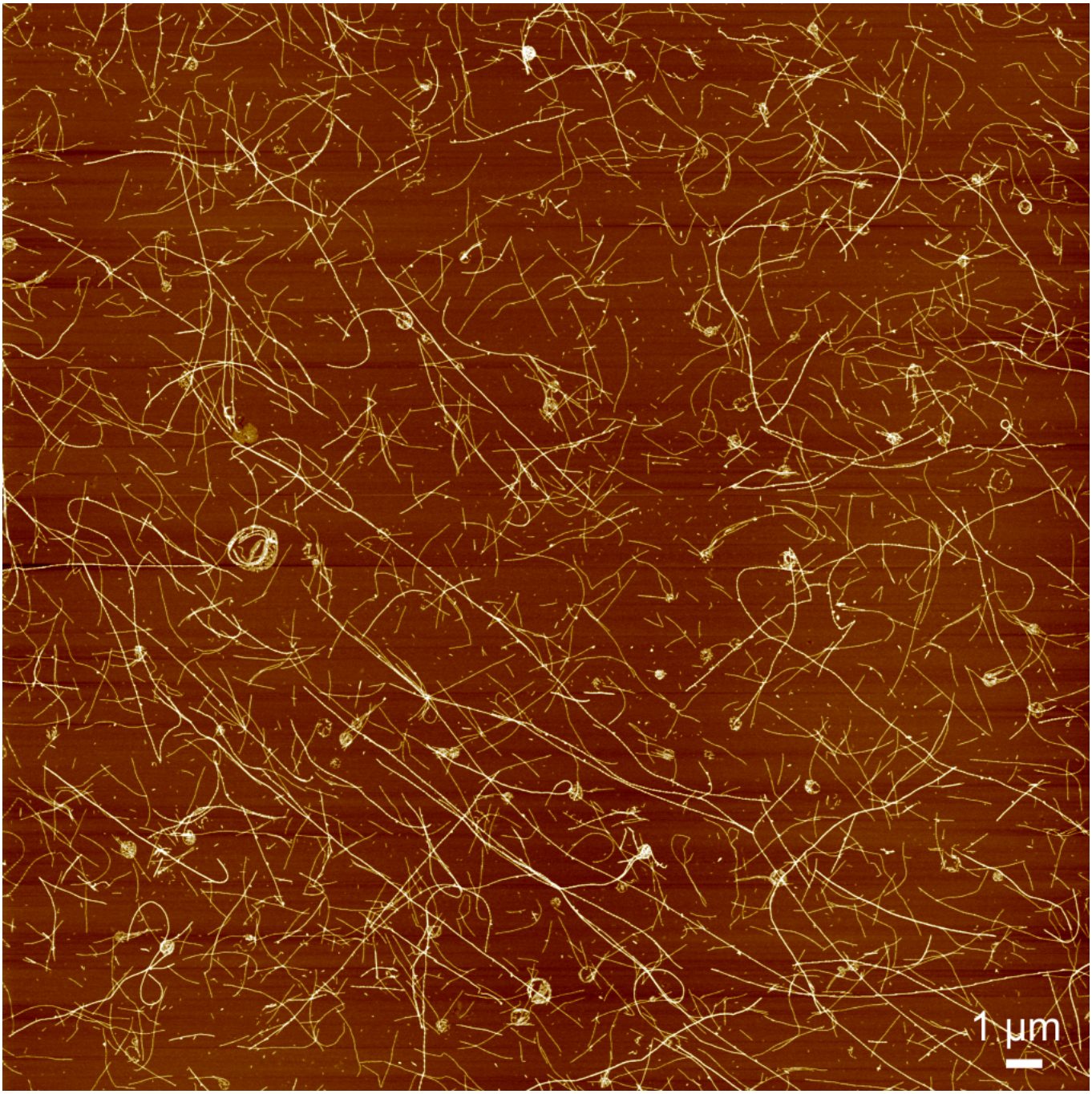

FIG. S7: Whole AFM image used for the curvature distribution analysis showing fibrils at the air-water interface after t=10 minutes adsorption time from a $c_{\mathrm{init}} = 0.001\%$ w/w fibril suspension.